LEGIBILITY NOTICE

A major purpose of the Technical Information Center is to provide the broadest dissemination possible of information contained in DOE's Research and Development Reports to business, industry, the academic community, and federal, state and local governments.

Although a small portion of this report is not reproducible, it is being made available to expedite the availability of information on the research discussed herein.

1

LA-UR ־89־325

TITLE: A DIFFUSION ACCELERATED SN TRANSPORT METHOD FOR
RADIATION TRANSPORT ON A GENERAL QUADRILATERAL MESH

LA-UR--89-325

DE89 007753

AUTHOR(S): R. E. ALCOUFFE

SUBMITTED TO: AMERICAN NUCLEAR SOCIETY TOPICAL MEETING
SANTA FE, NM - APRIL 9-13, 1989

DISCLAIMER

Los Alamos
Los Alamos National Laboratory
Los Alamos, New Mexico 87545

A Diffusion Accelerated Sn Transport Method for Radiation Transport on a General Quadrilateral Mesh

R. E. Alcouffe

X-6, MS B226
Los Alamos National Labo.atory
Los Alamos NM. 87545

Abstract

We present the development of a diffusion accelerated Sn transport method for the solution of temperature coupled radiation flow problems on a spatial mesh of arbitrary quadrilaterals in R-Z geometry. The diffusion acceleration equation is derived from the diamond-like transport spatial discretization. The effectiveness of the DSA method is shown on an example calculation and also computation times are indicated.

I. Introduction

Two-dimensional, time dependent radiation transport problems are frequently done on systems that are described by a general quadrilateral spatial mesh in R-Z geometry. A characteristic of thermal radiation transport problems is that in order to obtain a solution on reasonably large time steps, it is essential that the time differencing be completely implicit. In order to solve the implicit transport equation via the Sn method, both the usual inner and outer source iterations must be performed; and it is vital that an effective and efficient iteration accelerator be employed [1]. In this paper we describe the basic approach used to develop a diamond differenced representation for the Sn transport equation that is highly vectorized and hence computationally efficient on the Cray XMP's. We also describe a nonlinear version of the diffusion synthetic acceleration equation that works with the above Sn equation with good success. We conclude that we have developed a viable Sn transport method that is applicable to many problems in two dimensional thermal radiation flows.

II. Sn Spatial Solution on an Arbitrary Quadrilateral Mesh.

Given that we wish to describe the transport of radiation through a medium which exchanges energy with the radiation field through absorption, scattering, and emission processes, we can write the following set of equations:

$$\tau(I^{n+1} - I^n) + \Omega \cdot \nabla I(\mathbf{r}, v, \Omega) + \sigma_t(v, T_e) I(\mathbf{r}, v, \Omega) = \frac{1}{4\pi} \sigma_s(v, T_e) I_0(\mathbf{r}, v) +$$

$$\frac{1}{4\pi} \eta(T_e) X(v, T_e) \int_{4\pi} d\Omega' \int_0^\infty dv' \sigma_s(v', T_e) I(\mathbf{r}, v', \Omega') + Q(\mathbf{r}, v, \Omega) \tag{1}$$

$$\frac{\rho c}{\Delta t}(T_e^{n+1} - T_e^n) - \nabla \cdot k_e \nabla T_e(\mathbf{r}) = \int_0^\infty dv' \sigma_a(v', T_e) I_0(\mathbf{r}, v') - \sigma_p(T_e) u_e(\mathbf{r}) + S_e(\mathbf{r}) \tag{2}$$

where

$I^{n+1}(r, v, \Omega)$ is the radiation intensity at frequency v and angle Ω at time t^{n+1}.

$\sigma_a(v, T_e)$ is the absorption cross section at frequency v and temperature T_e.

$\sigma_s(v, T_e)$ is the scattering cross section at frequency v and temperature T_e.

$\sigma_t(v, T_e)$ $\sigma_a(v, T_e) + \sigma_s(v, T_e)$.

$X(v, T_e)$ $\sigma_a(v, T_e) b(v, T_e) / \sigma_p(T_e)$.

$\sigma_p(T_e)$ $\int \sigma_a(v, T_e) b(v, T_e) dv$.

u_e aT_e^4.

$b(v, T_e)$ is the normalized Planck function $(\int b(v, T_e) dv = 1)$.

τ $1/c\Delta t$.

k_e is the material conduction.

$\eta(T_e)$ is a derived function of the medium at temperature T_e, and $0 \leq \eta \leq 1$.

Q and S_e are extraneous sources of radiation and material energy respectively

The time discretization has been included in Eqn 1 so that it is apparent that the equation is solved completely implicitly in time for accuracy and stability considerations. Also Eqn 1 has been derived from the radiation transfer equation by including the effects of the medium upon the emission term. Our radiation transport problem consists in solving Eqn 1 over some time step to obtain the radiation intensity at the advanced time and then solving Eqn 2 to obtain the material

temperature. From the temperature, the cross sections and other quantities in Eqn. 1 are evaluated and the procedure is repeated for the next time step. In this work we focus on methods of solution of Eqn. 1 in two-dimensional R-Z geometry in which the spatial discretization consists of arbitrary quadrilaterals whose connectivity is logically rectangular.

We note that in general Eqn. 1 must be solved iteratively for the intensity and that analogous to transport calculations with fission, we have both inner iterations (to converge the scattering) and outer iterations (to converge the emission term). It is in the nature of radiation transport calculations that for large time steps the quantity $\eta(T_e)$ is very close to unity. Thus, the spectral radius of convergence of the outer iterations is also close to unity requiring many iterations for convergence; for most radiation flow problems, the number of iterations required for convergence at reasonable time steps is prohibitive. Thus a good acceleration method is required for convergence. In ref. 1 we outline in some detail for the orthogonal geometry case the diffusion acceleration method for radiation transport. In the next section of this paper, we detail how this is adapted for our non-orthogonal mesh.

We focus now on the question of finding the solution to Eqn. 1 on the non-orthogonal mesh for each iterate. Following Hill[2], we use his non iterative diamond difference-like approach to invert the left-hand side of equation 1 given that the right hand side is known. Referring to Fig. 1, the transport balance equation over spatial mesh cell (i,j) is written in the following form.

$$B_{i-1/2} \quad - \quad B_{i+1/2} \quad - \quad C_{j-1/2} \quad - \quad C_{j+1/2} \quad + A (\beta - \omega) =$$

$$(\sigma \quad) \quad - \quad (\sigma \quad_0) \quad + \quad (\quad) \quad + A \beta_{i,j}$$

where,

$$(3)$$

$$B_{i\pm1/2} \quad = \quad 2\pi(\mu A_{i\pm1/2} \quad - \quad \eta A_{i\pm1/2})_{i\pm1/2}$$

$$C_{i\pm1/2} \quad = \quad 2\pi(\eta A_{i\pm1/2} \quad - \quad \mu A_{i\pm1/2})_{i\pm1/2}$$

$$A_{i\pm1/2} \quad = \quad (\quad_{i\pm1/2} \quad_{i\pm1} \quad - \quad_{i\pm1/2} \quad_{i\pm1})$$

$$A_{i,j} \quad = \quad (\quad_{i\pm1/2} \quad_{i\pm1} \quad - \quad_{i\pm1/2} \quad_{i\pm1})$$

$$_{i,j} \quad = \quad (\quad_{i\pm1/2} \quad_{i\pm1} \quad + \quad_{i\pm1/2} \quad_{i\pm1}) / 2$$

This balance equation is then augmented by an appropriate diamond difference approximation.

relating the edge values to the cell centered values depending upon the number of sides visible. This method is supplemented by a set-to-zero fixup in case the angular intensity extrapolates to a negative value. As in the orthogonal case, the diamond differencing method is the simplest method having the diffusion limit. The simplicity allows for efficient coding with minimum storage requirements and the diffusion limit allows the accelerator to perform efficiently and yet obtain an accurate solution when the transport solution is diffusion-like. This certainly is an appropriate first attempt with the Sn method itself. In order to obtain a computationally efficient solution to Eqn. 3, we choose a space-angle sweeping sequence by means of an appropriate ordering scheme. The job of the ordering routine is to pick out the sequence of spatial meshes in an order which will allow the solver to invert the transport operator in a non-iterative manner. Since the transport operator is first order in both the spatial and angular derivatives, this can always be done. However, there is an additional task that the ordering routine must perform in order to take advantage of the architecture of the CRAY XMP computers. That is, since this is a vector machine, an ordering must be chosen so that the mesh sweeping can be vectorized for maximum solution speed on this machine. This means that groups of cells that can be solved simultaneously must be found by the ordering routine. On the logical mesh these cells will lie on diagonals.

We do the ordering on the logical mesh by typing cells as to how many sides are visible. Only two side visible cells can be efficiently solved simultaneously since they have a predictable stride as they do lie on the diagonals of the logical mesh. Operationally the ordering routine collects the following information (1) the starting cell number, (2) the starting cell type and (3) the number of cells in the diagonal. The mesh sweeper can then take this information, process it in order, and efficiently invert the transport operator on the vector machine. Thus the main difference between sweeping on a Lagrangian mesh and on an orthogonal mesh is making provisions in the mesh sweeper to solve one and three side visible quadrilaterals.

III. Diffusion Synthetic Acceleration of the Source Iteration

The diffusion acceleration method is a source iteration accelerator for radiation transport problems that involves the following ingredients (1) Formation of an appropriate diffusion equation whose solution is the same as the scalar intensity solution of the transport equation, (2) a solution method for inverting the resulting diffusion operator for each frequency group, and (3) an iteration method for solving the multigroup diffusion equation. For the general Lagrangian mesh case, it is not clear as yet what is the best method for addressing each of the above aspects.

Our experience in orthogonal mesh problems suggests that we derive the DSA equations by

forming the transport balance for the four mesh cells surrounding each vertex of the mesh. We develop our DSA equation in the non-orthogonal case in a manner analogous to that in our orthogonal development[1]. To sketch how this proceeds, we focus on the horizontal leakage terms in Eqn. 3; summing these terms for the four cells about vertex $(i+1/2, j+1/2)$, we have,

$$\mathcal{H}_{i+1/2,\,j+1/2} = ((\ddot{H})_{i+1/2} + (\ddot{H})_{i+3/2} + (\ddot{H})_{i+1/2,\,j+1} + (\ddot{H})_{i+1,\,j+1}$$

$$((\ddot{H})_{i/2} + (\ddot{H})_{i/2,\,j+1} + (\ddot{H})_{i+1/2,\,j+1} + (\ddot{H})_{i,\,j} \tag{4}$$

To derive our diffusion operator, we expand the angular flux in Eqn. 4 as a linear in angle function for each cell edge, namely,

$$\psi_{i+1/2}(\mu,\,\eta) = \psi_{0,\,i+1/2} + 3\ddot{H}_{i+1/2} \cdot \psi_{i+1/2}$$

$$\psi_{i+1/2}(\mu,\,\eta) = \psi_{0,\,i+1/2} + 3\ddot{\psi}_{i+1/2} \cdot F_{i+1/2} \tag{5}$$

where

$$\ddot{H}_{i+1/2} = \ddot{H}_{i+1/2} \Big/ \sqrt{A^2_{i+1/2} + B^2_{i+1/2}}$$

$$\ddot{\psi}_{i+1/2} = \ddot{\psi}_{i+1/2} \Big/ \sqrt{A^2_{i+1/2} + B^2_{i+1/2}}$$

and the A and B coefficients are found from the definitions in Eqn. 3.
Thus with this particular form for the expansion of the intensities on the cell edges, we have

$$\int_{4\pi} \psi_{i+1/2} \psi_{i+1/2} \, d\Omega \sqrt{A^2_{i+1/2} + B^2_{i+1/2}} \psi_{i+1/2} + \mathcal{A}_{i+1} \cdots$$

$$\int_{4\pi} \psi_{i+1/2} \psi_{i+1/2} \, d\Omega \, \mathcal{A}_{i+1/2} F_{i+1/2}$$

If we now substitute expansion (5) into Eqn. 4, we obtain the following diffusion expression for the horizontal leakage

$$\mathcal{H}_{i+1/2,\,j+1/2} ((\mathcal{A})_{i+1} + (\mathcal{A})_{i+3/2} + (\mathcal{A})_{i+1/2,\,j+1} + (\mathcal{A})_{i+1,\,j+1})$$

$$((\mathcal{A})_{i+1} + (\mathcal{A})_{i,\,j} + (\mathcal{A})_{i+1/2,\,j+1} + (\mathcal{A})_{i,\,j}) \tag{6}$$

To proceed further, we invoke some assumptions of linearity in Eqn 6, ie ,

$$(\mathcal{A})_{i-3/2} + (\mathcal{A})_{i-1/2} \equiv (\mathcal{A})_{i-1}$$

where

$$\mathcal{A}_{i-1} = \tfrac{1}{2}(\mathcal{A}_{i-3/2} + \mathcal{A}_{i-1/2})$$

$$(7)$$

If we further assume a Fick's law between the cell centered currents and the intensities, ie ,

$$\cdot = -\frac{\mathcal{A}}{3(\sigma \cdot)} \quad (\dot{\phi}_{0,i+1/2} - \dot{\phi}_{0,i-1/2})$$

$$(8)$$

then combining Eqns. 6,7 and 8, we obtain,

$$\mathcal{H}_{\dots} = -\frac{\mathcal{A}^2_{\dots}}{3(\sigma \cdot)}_{\dots} (\cdot_{\dots} - \cdot_{\dots}) - \frac{\mathcal{A}^2_{\dots}}{3(\sigma \cdot)}_{\dots} (\cdot_{\dots} - \cdot_{\dots}) \cdot$$

$$\frac{\mathcal{A}^2_{\dots}}{3(\sigma \cdot)}_{\dots} (\cdot_{\dots} - \cdot_{\dots}) \cdot \frac{\mathcal{A}^2_{\dots}}{3(\sigma \cdot)} (\cdot_{\dots} - \cdot_{\dots})$$

$$(9)$$

Because Eqn 9 is in terms of cell edge quantities, it still is not suited for efficient solution with known methods, thus, we make a further approximation. The most straightforward one is that analogous to diamond, ie., we set

$$\dot{\phi}_{0,i+1/2,\cdot} = \tfrac{1}{2}(\dot{\phi}_{0,i+1/2,\cdot+1/2} + \dot{\phi}_{0,i+1/2,\cdot-1/2})$$

Substituting this form into Eqn. 9 leads to a nine point form for the diffusion operator which is to be expected for a general quadrilateral mesh. However, if our experience from the orthogonal case is at all relevant, then frequently it is not necessary to employ such an elaborate diffusion operator. This is because the correction term from the transport solution allows the DSA equation to be accurate for a lower order operator. That is, it may be possible to go to a five point operator, which is much less costly to solve, and still have the accelerator be effective in many of the cases we encounter in practice. A five point form that can be approximated from Eqn 9 is.

$$\mathcal{H}_{\ldots\ldots} = -D_{\ldots\ldots}(\zeta_{\ldots\ldots} - \zeta_{\ldots\ldots}) + D_{\ldots\ldots}(\zeta_{\ldots\ldots} \ldots)$$

where

$$D_{\ldots} = \frac{1}{2}\frac{\lambda^2}{3(\sigma^2)_{\ldots}} + \frac{\lambda^2}{3(\sigma^2)}$$

(10)

The vertical leakage terms are derived in an analogous way, and thus our five point form for the DSA equation for a general quadrilateral mesh is written as:

$$-D_{i,\ i,\ -1/2}(\zeta_{0,\ -3/2,\ -1/2} - \zeta_{0,\ -1/2,\ -1/2}) + D_{i,\ 1/2}(\zeta_{0,\ -1/2,\ -1/2} - \zeta_{i,\ 2,\ -1/2}) -$$

$$-D_{i,\ 1/2,\ -1}(\zeta_{0,\ -1/2,\ -3/2} - \zeta_{0,\ -1/2,\ -1/2}) + D_{i,\ 1/2,}(\zeta_{0,\ -1/2,\ -1/2} - \zeta_{-1,\ 2,\ i,\ 2}) +$$

$$(\sigma^2)_{\ldots}\zeta_{0,\ 1/2,\ -1/2} = (S^2)_{\ldots} + (\mathcal{H}_{i,\ 1/2,\ -1/2} + \mathcal{V}_{i,\ 2,\ -1/2}$$

$$-\mathcal{H}_{-1/2,\ -1/2} \quad \mathcal{V}_{i,\ 1/2,\ -1/2})$$

(11)

where

$\mathcal{H}^1$ and $\mathcal{V}^1$ are the angle integrated form of Eqn 4 employing the solution to Eqn 3, $I^1(\mu,\eta)$.

$(\sigma_R V)_{\ldots}$ is, the sum of the four cell removal divided by $V_{\ldots}$.

Eqn 11 is used to accelerate the source iteration of Eqn 3 and it is easily shown that upon convergence, the solution of Eqn 11 is the same as the angle integrated solution to Eqn 3. To invert the diffusion operator of Eqn 11, we use our multigrid solver already implemented for the orthogonal case since it is very efficient for the five point form. Thus Eqn 11 serves as the basis for the acceleration of the iterations required in the solution of the radiation transport equation.

As noted in ref 1, the multifrequency diffusion iterations must themselves be accelerated, we use the same grey approach outlined in that reference.

It should be obvious by now that the success of the above outlined transport solution method is highly dependent upon the representation of the diffusion acceleration equation as a five point operator. This five point representation is not an essential restriction but it certainly does simplify the

the implementation of the method for Lagrange meshes. We use the example problem presented below to demonstrate the effectiveness of the DSA as described above as well as to give an indication of the accuracy of the Sn method itself on non-orthogonal meshes.

IV. Calculational Results

The method described above for solving the temperature coupled radiation transport equation has been encoded in a special version of the TWODANT[3] code which we call SHORTIE. This includes the time step control, temperature calculation, cross section generation, and iteration acceleration within each time step as well as the mesh ordering and sweeping algorithms for the nonorthogonal mesh. All of the computational parts are vectorized so that the method can be run efficiently on our CRAY XMP 48 computers. In this section we address the computational time and iteration efficiency from our experience with the code so far on model type problems, and we demonstrate the accuracy of the basic transport method on a problem in radiation flow.

On model problems, our experience has shown that the solution time per phase space cell on an orthogonal mesh with negative flux fixup using an XMP 48 is from 0.7 to 1.0 microseconds CPU time in TWODANT. We have benchmarked the nonorthogonal solver in SHORTIE for similar model problems at from 1.2 to 3.0 microseconds per cell. The range of solution times reflects the fact that the solution time is a strong function of the number of 'special' cells that have to be calculated; ie. the one and three side visible cells. The upper limit is representative of a highly disordered mesh in which 30-40% of the cells are special. These time do demonstrate that the vectorization of the sweeping algorithm is successful and compares favorably with the highly efficient TWODANT module.

Our experience with the DSA accelerator for nonorthogonal meshes shows that it can be just as effective as the DSA accelerator in the orthogonal case. But it also suffers from the same limitations as the TWODANT accelerator in that its effectiveness decreases as the number of negative flux fixups increase or as the size of the mesh in mfp increases. Thus, although it is difficult to generalize, it can be said that for many typical radiation flow problems the DSA accelerator is as effective as the orthogonal one. For example, in the below described problem, we require on the average only two transport iterations per time step to reduce the error in the emission source by an order of magnitude while the time step varied from 0.001 to 1.0 ns.

Our example radiation flow problem consists of a homogeneous cylinder, 9 cm in radius and 9 cm in height. The radiating medium is modeled as polyethelene at a density of 0.05 g/cc. A uniform source of radiation impinges on the bottom of the cylinder at time zero. The source is

assumed isotropic and Planckian with a temperature of 1 KeV. The task is to compute the evolution of the material temperature as a function of time and position until equilibrium is attained (there is no material motion). We chose to solve this problem using 10 frequency groups equilogarithmically distributed between 0.005 to 20 KeV; the material initial temperature is 0.05 KeV. In the first (highest energy) four groups, we use an S8 quadrature (standard TWODANT) and in the remaining groups, S4. The given spatial calculational mesh is shown in Fig. 2 where the radius increases along the vertical axis and the z axis is horizontal (the source impinges on the left side of the figure). There are 48x48 mesh intervals in this problem. As can be seen, this is a highly distorted mesh that has been seen a great deal in the literature and has been used to challenge diffusion solvers. In order to have a reference calculation, we made a varient of this problem with a uniform, orthogonal mesh which turns out to be perfectly square in R-Z geometry and hence is nearly ideal for a benchmark.

In Figs. 3a-3d, we present contour plots of the material temperature at selected times; the last time, 30 ns, being the time at which the system attains equilibrium. Each plot is actually of two sets of contours, one from the mesh of Fig.2 and the other from the orthogonal mesh. Inspection of the plots shows that the orthogonal and nonorthogonal results match remarkably well. The aberrations in the nonorthogonal results are at the positions where one would expect fixup effects to be important. We also note that the computation times and iteration patterns are very close to the same confirming that the accelerator is performing equally as well in both cases.

V. Remarks and Conclusions

We have developed a diffusion synthetic accelerated transport solver on a general quadrilateral mesh that performs well on radiation transport problems. The development of the accelerator follows the same kind of logic used to develop the original orthogonal one and seems to perform in relatively simple radiation flow problems equally as well. Will this be applicable to conventional neutral particle transport as well? There is no theoretical reason why not except in the case of eigenvalue problems. Here we would need to develop some kind of diffusion correction scheme in order to have a compatible outer iteration accelerator. In this case it may be possible that the five point form would be a severe limitation. However from these results of radiation transport, it appears that it is worthwhile to pursue a general geometry TWODANT.

VI. References

1. RE Alccuffe, BA Clark and EW Larsen, "The Diffusion Synthetic Acceleration of Transport Iterations with Application to a Radiation Hydrodynamics Problem", Multiple Time Scales, Accdemic Press, Inc (1985)

2. TR Hill and RP. Paternoster, "Two-Dimensional Spatial Discretization Methods on a Lagrangian Mesh", Los Alamos/CEA Meeting on Deterministic Transport Methods, Bruyers-le-Chatel, France (1982)

3. RE Alcouffe, FW Brinkley, DR Marr, RD O'Dell, "User's Guide for TWODANT: A CodePackage for Two-Dimensional, Diffusion-Accelerated Neutral Particle Transport", LA-10049-M, Los Alamos National Lab, 1984

Fig. 1. Reference Quadrilateral for hte Development of the Transport Balance Equation.

Fig. 2. R-Z Mesh Arrangement for the Example Radiation Flow Problem.

Fig. 3a. Contour Plot of .he Material Temperature at Time = 2.0 ns.

Fig. 3b. Contour Plot of the Material Temperature at Time = 4.0 ns.

Fig. 3c. Contour Plot of the Material Temperature at Time = 10.0 ns.

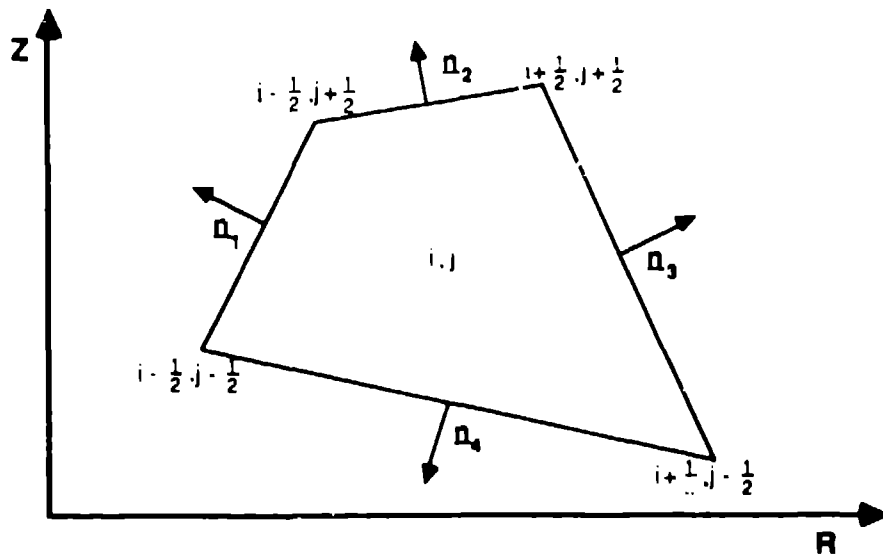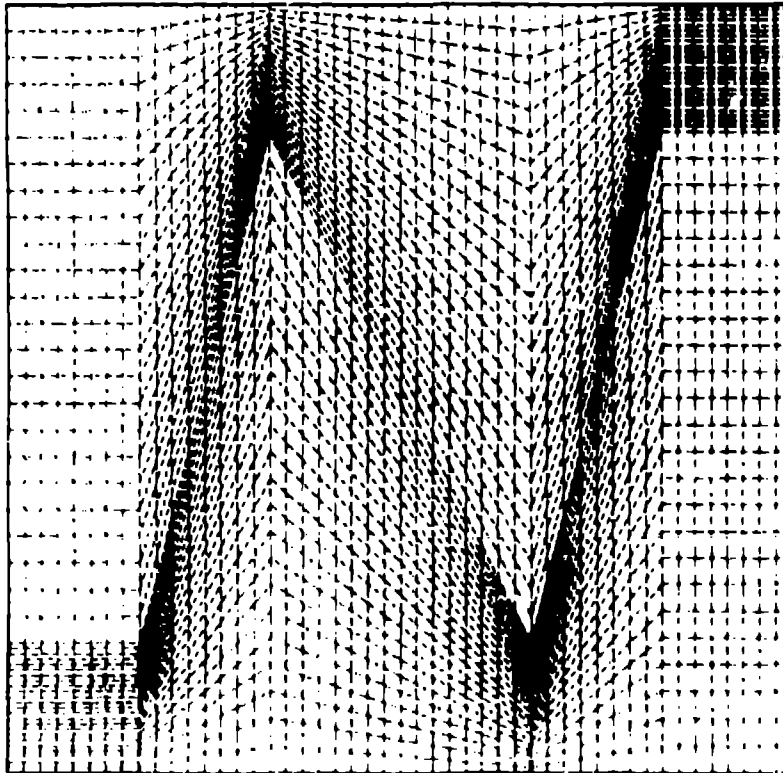Fig. 3d. Contour Plot of the Material Temperature at Time = 30.0 ns.

Fig. 1. Reference Quadrilateral for the Development of the Transport Balance Equation.

Fig. 2. R-Z Mesh Arrangement for the Example Radiation Flow Problem.

Time = 2.0 ns

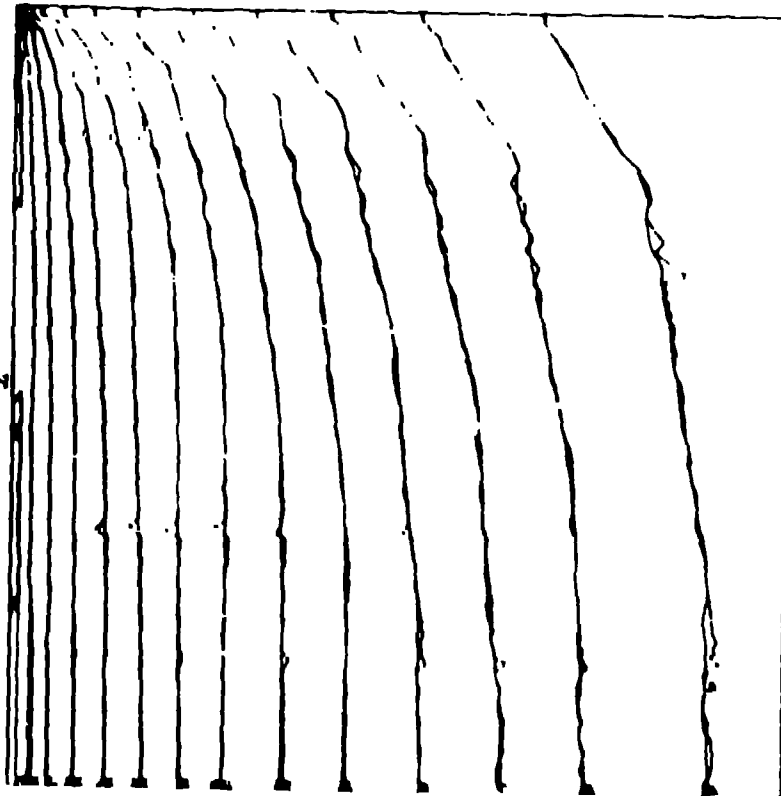Fig. 3a. Contour Plot of the Material Temperature at Time = 2.0 ns.

Time   4.0 ns

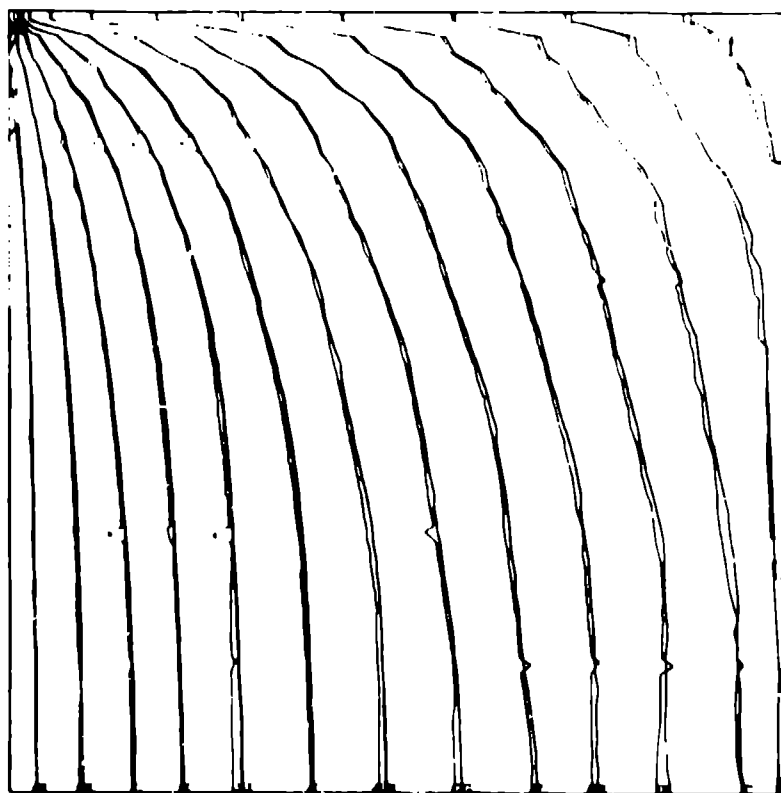Fig. 3b. Contour Plot of the Material Temperature at Time = 4.0 ns.

Time   10.0 ns

Fig. 3c. Contour Plot of the Material Temperature at Time = 10.0 ns.
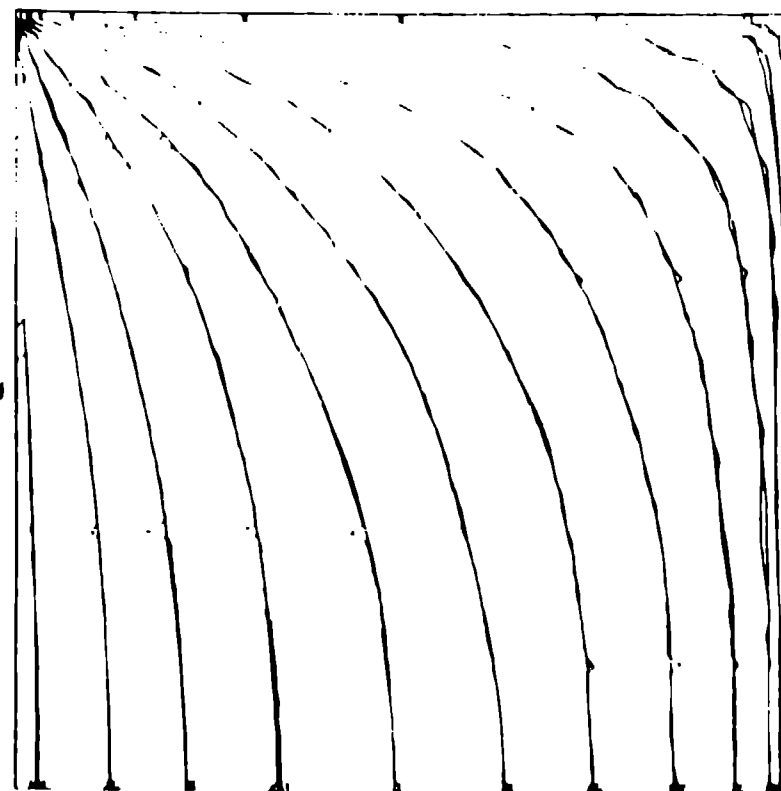

Time −30.0 ns

Fig. 3d. Contour Plot of the Material Temperature at Time = 30.0 ns.